Biochemistry **2005,** *44,* 2163−2172

Duplex and Quadruplex DNA Binding and Photocleavage by Trioxatriangulenium Ion[†]

Arti Pothukuchy,[‡] Carolyn L. Mazzitelli,[§] Mireya L. Rodriguez,[‡] Bodin Tuesuwan,[‡] Miguel Salazar,[‡]
Jennifer S. Brodbelt,[*,§] and Sean M. Kerwin[*,‡]

Division of Medicinal Chemistry and Institute for Cellular and Molecular Biology and Department of Chemistry and Biochemistry, The University of Texas, Austin, Texas 78712

Received July 2, 2004; Revised Manuscript Received October 22, 2004

ABSTRACT: The stable trioxatriangulenium ion (TOTA) has previously been shown to bind to and photooxidize duplex DNA, leading to cleavage at G residues, particularly 5′-GG-3′ repeats. Telomeric DNA consists of G-rich sequences that may exist in either duplex or G-quadruplex forms. We have employed electrospray ionization mass spectrometry (ESI-MS) to investigate the interactions between TOTA and duplex DNA or G-quadruplex DNA. A variety of duplex decamer oligodeoxynucleotides form complexes with TOTA that can be detected by ESI-MS, and the stoichiometry and fragmentation patterns observed are commensurate with an intercalative binding mode. TOTA also forms complexes with four-stranded and hairpin-dimer G-quadruplex oligodeoxynucleotides that can be detected by ESI-MS. Both the stoichiometry and the fragmentation patterns observed by ESI-MS are different than those observed for G-tetrad end-stacking binding ligands. We have carried out ^{1}H NMR titrations of a four-stranded G-quadruplex in the presence of TOTA. Addition of up to 1 equiv of TOTA is accompanied by pronounced upfield shifts of the G-tetrad imino proton resonances in the NMR, which is similar to the effect observed for G-tetrad end-stacking ligands. At higher ratios of added TOTA, there is evidence for additional binding modes. Duplex DNA containing either human telomeric repeats $(T_2AG_3)_4$ or the *Tetrahymena* telomeric repeats $(T_2G_4)_4$ are readily photooxidized by TOTA, the major sites of oxidation being the central guanine residues in each telomeric repeat. These telomeric repeats were incorporated into duplex/quadruplex chimeras in which the repeats adopt a G-quadruplex structure. Analysis by denaturing polyacrylamide gel electrophoresis reveals significantly less TOTA photocleavage of these quadruplex telomeric repeats when compared to the duplex repeats.

Oxidative damage to DNA may involve long-range charge transport, such that the ultimate DNA lesion can be far removed from the original oxidant (*1*−*3*). The facility of charge transport through duplex DNA may be modulated through structural changes that affect DNA base stacking (*4*). Guanine is the DNA base that is most easily oxidized, and within duplex DNA adjacent deoxyguanosines are even more readily oxidized than base-paired deoxyguanosine residues flanked by other nucleotides (*5*). The radical cation that is generated upon G-residue oxidation in duplex DNA leads to base-labile sites that can be readily detected by treatment of the DNA with hot piperidine, resulting in DNA strand cleavage (*6*). The ease with which a given guanosine within a run of G-residues in duplex DNA is cleaved as a result of oxidation is a function of a flanking sequence (*7*). Thus far, only limited studies on the effect of higher-order DNA structure on electron transport and guanosine oxidative cleavage have been reported (*8*−*11*).

It has been proposed that G-rich regions of DNA may serve as cathodic protection for intervening DNA sequences; for example, in humans the intron regions are rich in guanosine, and these regions possibly protect the exons from oxidative damage (*12*). Telomeres are the structures present at the end of chromosomes and are composed of tandem repeats of short, G-rich DNA sequences (*13*). It is known that these structures are essential for chromosome stability and the complete replication of the chromosomal terminus for each cell cycle (*14*). Since telomeric regions are also rich in guanosine, they may also play a role in protecting the genome from oxidative damage (*15*).

G-rich DNA sequences can adopt unusual structures, in which Hoogsteen hydrogen bonded G-tetrads stack upon each other to form four-stranded assemblies called G-quadruplex DNA (*16*). Telomeric DNA (*13*, *17*, *18*) and other G-rich DNA sequences (*19*) have been proposed to form G-quadruplex DNA structures or other higher-order DNA structures (*20*). However, the role of the structure of telomeric DNA (e.g., duplex vs quadruplex) on its ease of oxidation has not been widely explored (*10*).

The trioxatriangulenium ion, TOTA,[1] is a stable, planar carbocation that has recently been the subject of theoretical (*21*), structural (*22*), and photophysical (*23*) studies. We have previously shown that TOTA can effect photochemical cleavage of duplex DNA (*24*). The preferential cleavage of

---

[†] This work was supported by grants from the Robert A. Welch Foundation (F-1298 to S.M.K. and F-1155 to J.S.B.) and the National Institutes of Health (RO1 GM65956 and ES 07784).

[*] Corresponding authors. (S.M.K.) E-mail: skerwin@mail.utexas.edu. Tel: (512) 471-5074. Fax: (512) 232-2606. (J.S.B.) E-mail: jbrodbelt@mail.utexas.edu. Tel: (512) 471-0028.

[‡] Division of Medicinal Chemistry and Institute for Cellular and Molecular Biology.

[§] Department of Chemistry and Biochemistry.

10.1021/bi0485981 CCC: \$30.25

Table 1: DNA Sequences Used in This Paper

TG	5′-GCTGCGTCCAACTATGTATAC-$(\mathrm{T_2G_4})_4$TT-AGCGGCACGCAATTGCTATAGTGAGTCGTATTA-3′
TAG	5′-GCTGCGTCCAACTATGTATAC-$(\mathrm{T_2AG_3})_4$TT-AGCGGCACGCAATTGCTATAGTGAGTCGTATTA-3′
T6	5′-TAATACGACTCACTATAGCAATTGCGTGCCGCT-$\mathrm{T_6}$-GTATACATAGTTGGACGCAGC-3′
CTA	5′-TAATACGACTCACTATAGCAATTGCGTGCCGCT-AA$(\mathrm{C_3TA_2})_4$-GTATACATAGTTGGACGCAGC-3′
CA	5′-TAATACGACTCACTATAGCAATTGCGTGCCGCT-AA$(\mathrm{C_4A_2})_4$-GTATACATAGTTGGACGCAGC-3′
G3	5′-TTAGGGTTAGGGTTAGGGTTAGGG-3′
G4	5′-TTGGGGTTGGGGTTGGGGTTGGGG-3′
D12	5′-CGCGAATTCGCG-3′
D10A1	5′-GCGCATGCGC-3′
D10A2	5′-GCGATATCGC-3′
D10A3	5′-GCATATATCG-3′
G5	5′-TTGGGGGT-3′
G2	5′-TTAGGGTTAGGG-3′
G1	5′-TAGGGTTA-3′

Table 2: Summary of CAD Results

	duplex/TOTA complexes (−4)[a]	duplex/TOTA complexes (−5, −6)[a]	quadruplex/TOTA complexes (−6, −7)[a]
major fragmentation pathway	base loss[b]	strand separation[c]	strand separation[c]
moderate fragmentation pathway	strand separation[c]	N/A	fragmentation of ss backbone[d]
minor fragmentation pathway	fragmentation of ss backbone[d]	N/A	base loss (−GH)

[a] Values in parentheses indicate charge states. [b] Indicates loss of nucleobase(s) from parent complex. [c] Unzipping of duplex or quadruplex to produce single strand (ss) ODNs. [d] Production of *w* and ($a - B$) ions.

5′-Gs in 5′-GG-3′ dinucleotide steps after piperidine heat treatment, and the equal photochemical cleavage efficiency in H_2O and D_2O, have been cited as evidence for the formation of guanine radical cations by electron transfer from DNA to photoexcited TOTA (*24*). Subsequently, Schuster and co-workers reported the X-ray structure of TOTA intercalated into duplex DNA and confirmed the ability of the photochemically excited TOTA to undergo electron transfer leading to guanine radical cations (*25*). The ability of TOTA to photooxidize duplex DNA, and its structural similarity to known polycyclic quadruplex DNA binding agents (*26*), led to the current investigation of the interaction of this stable cation with duplex and quadruplex DNA structures. DNA binding and photocleavage by TOTA is revealed by PAGE, UV/vis spectrophotometry, ^{1}H NMR, and electrospray ionization mass spectrometry (ESI-MS). The investigation of the ability of duplex and quadruplex DNA to undergo photochemical oxidation by TOTA may shed light on the effect of higher order telomeric DNA structures on the potential cathodic protection afforded by these sequences.

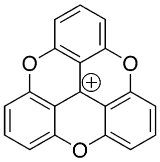

TOTA$^{\oplus}$

ESI-MS has emerged as a useful technique to examine interactions between small molecules and nucleic acids as a result of its low sample consumption and fast analysis time, making it adaptable to high throughput screening techniques (*27*, *28*). ESI allows noncovalent complexes in solution to be gently lifted to the gas phase while maintaining many of the binding interactions. The preservation of these noncovalent complexes allows information about binding stoichiometry and selectivity to be elucidated from the mass spectra. Additionally, collisional activated dissociation (CAD) (*29*) experiments can be performed on selected complexes to evaluate their stabilities and binding modes as a function of characteristic fragmentation patterns (*30*−*33*).

The majority of past ESI-MS studies of DNA/drug complexes have examined the binding of well-studied duplex−interactive drugs, including the minor groove binding distamycins and intercalating anthracyclines (*27*, *28*). There is significant evidence from these studies that the behavior of the complexes in the gas-phase can be correlated to that of solution (*34*). Recently, studies by our group and others have extended the use of ESI-MS to investigate complexes formed between G-quadruplex DNA and drug molecules (*35*−*39*).

Here, we investigate the complexation and photooxidation of duplex and G-quadruplex DNA with TOTA. ESI-MS is used to probe the selectivity and binding mode of TOTA with duplex and quadruplex DNA. Although TOTA does not display any selectivity for binding to duplex versus quadruplex DNA, the photochemical cleavage of these two DNA structures by TOTA is remarkably different. We show that 5′-GGG-3′ triads and 5′-GGGG-3′ tetrads in duplex DNA consisting of telomeric T_2AG_3 or T_2G_4 repeats are preferentially photocleaved with a characteristic pattern, in agreement with previous observations of guanine radical cation trapping. The pattern and extent of photocleavage, however, changes when these 5′-GGG-3′ triads and 5′-GGGG-3′ tetrads form G-quadruplex structures.

EXPERIMENTAL PROCEDURES

Oligonucleotides **TAG**, **TG**, **T6**, **CTA**, **CA**, **G3**, **G4**, and **D12** (Table 1) were synthesized in-house on an automated DNA synthesizer using standard phosphoramidite coupling and purified by denaturing polyacrylamide gel electrophore-

---

[1] Abbreviations: CAD, collisional activated dissociation; DMS, dimethyl sulfate; ESI-MS, electrospray ionization mass spectrometry; ODN, oligodeoxynucleotide; PAGE, polyacrylamide gel electrophoresis; Tris, *N*,*N*,*N*-tris(hydroxymethyl)aminomethane; TOTA, trioxatriangulenium ion.

sis. Ammonium salts of self-complementary oligonucleotides **D10A1**, **D10A2**, and **D10A3** (Table 1) and G-quadruplex forming oligonucleotides **G2** and **G5** (Table 1) were purchased from TriLink Biotechnologies Inc. (San Diego, CA) and custom synthesized on the 1.0 μmol scale with purification by reversed-phase HPLC. The perchlorate salt of TOTA (*23*) was a gift from Karickal Gopidas (CSIR, Trivandrum, India).

Preparation of ^{32}P-Radiolabeled Duplex and Quadruplex Oligonucleotides. The DNA strands **TAG** and **TG** were 5′-labeled with [γ-^{32}P]-ATP (Amersham) using T4 polynucleotide kinase (New England Biolabs). For G-quadruplex constructs, these labeled DNA strands were denatured by being heated to 95 °C for 5 min in a buffer consisting of 10 mM Tris HCl (pH 8.0) and 100 mM KCl. The samples were then allowed to cool slowly to room temperature, then kept at 4 °C overnight. The complementary strand (**T6**, 3-fold molar excess) was then added, and the mixture was incubated at 55 °C for 1 h and allowed to cool slowly to room temperature. For duplex substrates, labeled G-rich DNA strands (**TAG** or **TG**) were mixed with the complementary strands (**CTA** or **CA**, 3-fold molar excess) at 95 °C for 5 min in the Tris-KCl buffer. The samples were allowed to cool to room temperature overnight. All DNA substrates were further purified by 8% nondenaturing PAGE and subsequently stored at 4 °C in Tris-KCl buffer. DMS footprinting of the G-quadruplex and duplex substrates was carried out to confirm the formation of the indicated DNA structures, both in the presence and in the absence of added TOTA (Supporting Information).

DNA Photocleavage Reactions. Reaction mixtures (20 μL total volume) containing 5′-labeled DNA substrate (30 000 cpm, ~300 fmol), 10 μM TOTA perchlorate, and 100 mM KCl in 50 mM sodium phosphate buffer (pH 7.0) were irradiated at room temperature in an LZC-4 photo reactor (Luzchem) equipped with UVA lamps (350 nm) for 30 min. Immediately after irradiation, the reaction mixtures were treated with stop buffer consisting of 0.1 M thiourea, 0.3 M sodium acetate (pH 5.2), and 10 μg of tRNA. The samples were then subjected to ethanol precipitation. After the DNA was pelleted, samples were washed with 70% ethanol and dried. These samples were then subjected to piperidine heat treatment (1 M piperidine, 90 °C, 15 min). The cleaved products were finally resolved on 12% denaturing PAGE and visualized and quantified using a phosphorimager.

Mass Spectrometry. Solutions containing the quadruplex-forming ODNs (**G5** and **G2**) were prepared in 150 mM ammonium acetate and annealed by being heated to 90 °C and slowly cooling to room temperature during a period of 7−8 h. The self-complementary duplex-forming ODNs (**D10A1**, **D10A2**, and **D10A3**) were annealed in a 250 mM ammonium acetate solution by being heated to 90 °C and slowly cooling to room temperature during a period of 2−3 h. Analytical solutions were prepared containing the quadruplex or duplex DNA and TOTA perchlorate, each at equal 10 μM concentrations in 3:1 25 mM ammonium acetate/methanol. The solutions were directly infused into a ThermoFinnigan LCQ Duo mass spectrometer (San Jose, CA) using a Harvard syringe pump (Holliston, MA) set at 3 μL/min. The ESI source was operated in the negative ion mode with an electrospray voltage of 3.5 kV and a heated capillary temperature of 90 °C. Nitrogen sheath and auxiliary gas set at 40 and 10 arbitrary units, respectively, were used to aid in desolvation. Each spectrum was acquired using an ionization time of 100−250 ms, and an acquisition of 300 scans was averaged. The base pressure of the trap was set at $\sim 1 \times 10^{-5}$ Torr. Collisional activated dissociation (CAD) experiments were performed on selected DNA/TOTA complexes by isolating the desired precursor ion in the trap using resonance ejection, followed by increasing the collision energy applied to the trap to produce fragmentation.

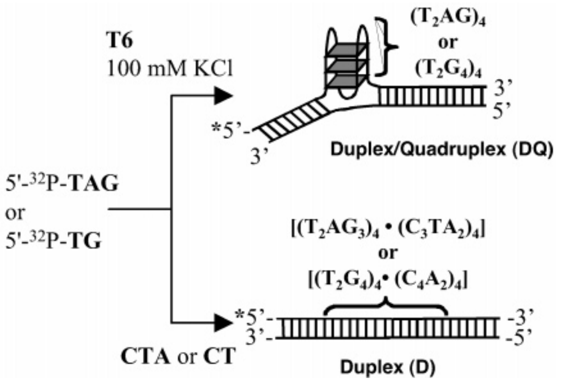

FIGURE 1: Structures of 5′-labeled duplex telomeric DNA (D, bottom) or chimera duplex-quadruplex telomeric (DQ, top) structures used in this work.

UV/Vis Spectroscopy. The buffer used for this study was 10 mM sodium phosphate (pH 7) containing 100 mM KCl. The DNA concentration for all the samples was 5 μM. All the DNA samples were dissolved in sodium phosphate buffer (10 mM, pH 7) containing 100 mM KCl. Samples were heated to 95 °C for 5 min, cooled to room temperature, and kept at 4 °C overnight. DNA samples were then incubated with 10 μM TOTA perchlorate, and the spectra were recorded on a Cary 100 spectrophotometer in 310−380 nm range.

NMR Spectroscopy. ODN **G1** was synthesized in-house on an automated DNA synthesizer using standard phosphoramidite coupling and purified by reversed-phase HPLC. After dialysis against deionized water and lyophilization, the G1 sample was dissolved (3.23 mM strand) in 90% H_2O/10% D_2O containing 150 mM KCl, 25 mM potassium phosphate, and 1 mM EDTA (pH 7) and heated to 90 °C for 5 min. The DNA solution was allowed to cool slowly to room temperature over 48 h to form the quadruplex DNA structure. ^{1}H NMR spectra were recorded at 27 °C utilizing a standard jump-return pulse sequence for water suppression (*40*) with a relaxation delay of 2 s. These spectra indicated the ODN had formed a parallel-strand G-quadruplex structure, as evidenced by the diagnostic imino proton resonances at 10−12 ppm. This sample was then titrated with a solution of TOTA perchlorate in DMSO (60 mM), and ^{1}H NMR spectra were recorded after each addition.

RESULTS

Table 1 shows the sequences of the various oligodeoxynucleotide (ODN) sequences used in this work. We have previously demonstrated that the 5′-end-labeled ODNs **TAG** and **TG** can each be hybridized to the unlabled oligomer **T6** in 100 mM KCl-containing buffer to form stable chimeras consisting of a duplex structure with a G-quadruplex structure near the center of the duplex (Figure 1) (*41*). Gel mobility

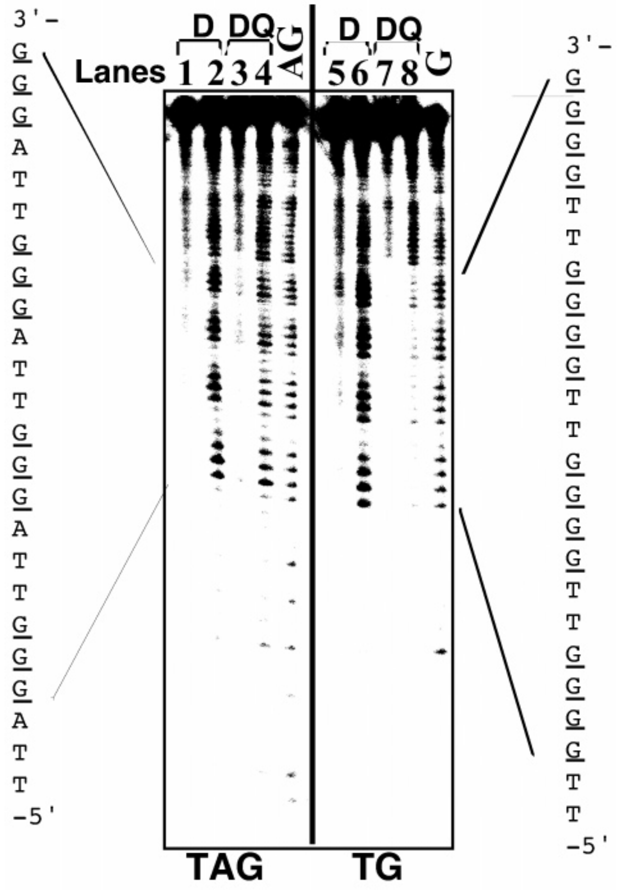

FIGURE 2: Phosphorimage of the DNA photocleavage product for the top strands of the TAG and TG duplex (D) and quadruplex (DQ) substrates in the presence of 10 μM TOTA, 100 mM KCl phosphate buffer pH 7.0, after irradiation (350 nm, 30 min). Lanes 2, 4, 6, and 8 are DNA photocleavage mixtures following piperidine heat treatment. Lanes 1, 3, 5, and 7 are DNA photocleavage mixtures without subsequent piperidine heat treatment. Lanes AG and G are Maxam and Gilbert sequencing lanes.

shifts and DMS footprinting demonstrate that the human telomere repeat sequence T_2AG_3 (in the case of **TAG•T6**) or the *Tetrahymena* telomere repeat sequence T_2G_4 (in the case of **TG•T6**) in these chimeras form quadruplex structures (ref *41* and Supporting Information). In both cases, the bottom **T6** strand contains six unpaired T-residues that bridge the G-quadruplex region. DMS footprinting of these two chimeras carried out in the presence of TOTA demonstrates that the T_2AG_3 and T_2G_4 repeats remain in a quadruplex form (Supporting Information). One advantage of this type of construct is that one can study DNA cleavage chemistry of both duplex and G-quadruplex DNA structures within the same substrate (*41*). However, to study the photochemical cleavage of these telomeric repeats in a duplex DNA context, we carried out the hybridization of 5′-end-labeled **TAG** or **TG** with their complementary strands, **CTA** or **CA**, respectively (Figure 1).

Evaluation of Photochemical Cleavage. The 5′-end labeled chimeric duplex/quadruplex and the duplex substrates (Figure 1) were irradiated in a photochemical reactor with UVA light (~350 nm) for 30 min in the presence of 10 μM TOTA. Denaturing polyacrylamide gel electrophoresis of the DNA products before and after piperidine heat treatment (Figure 2) demonstrates that TOTA produces significant photochemical cleavage of the DNA only after piperidine heat treatment, with cleavage occurring primarily at G-residues. Control reactions indicate that neither light nor TOTA alone causes appreciable DNA strand scission, either before or after piperidine heat treatment (Supporting Information). The extent of photochemical DNA cleavage by TOTA is not uniform. In the duplex substrate containing the human telomeric repeat T_2AG_3, the central guanosine in the T_2AG_3 repeat is cleaved preferentially. This is more evident in Figure 3A, which shows the quantification of the DNA cleavage of lane 2 in Figure 2. The photochemical oxidation of 5′-GGG-3′ repeats is reported to be dependent on the flanking sequence (*18*, *42*). Previous studies of the photochemical oxidation of duplex T_2AG_3 repeats with riboflavin also demonstrated preferential cleavage of the central guanosine residue (*7b*). The **TOTA** photochemical cleavage of the duplex DNA substrate containing the *Tetrahymena* telomeric repeat T_2G_4 results in slight preferential cleavage of the

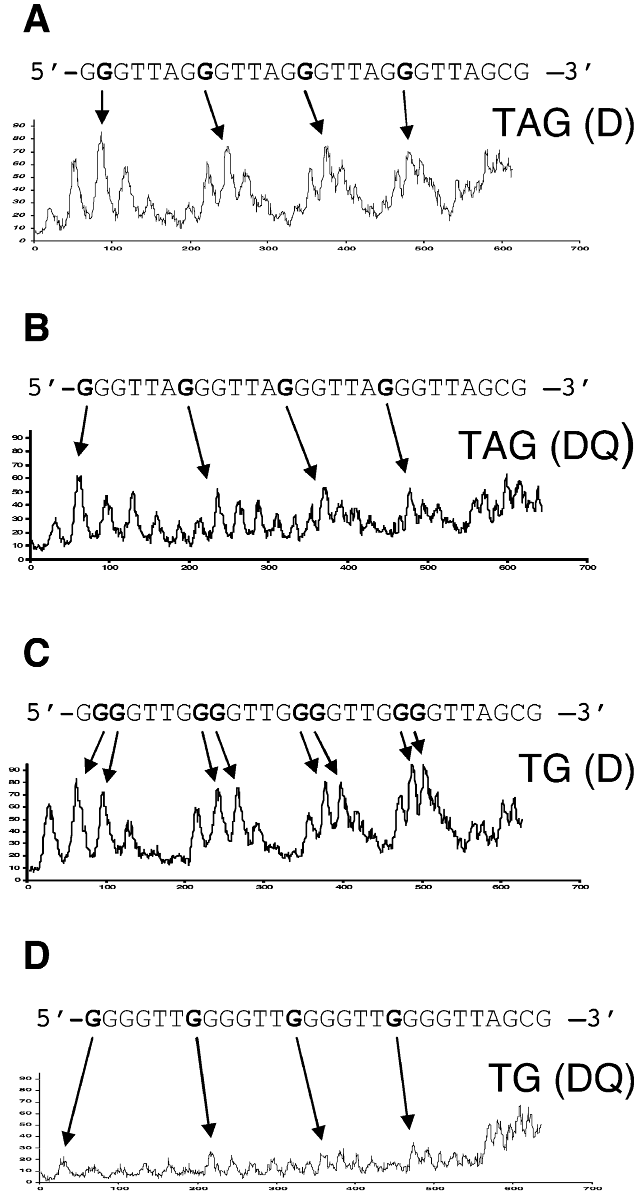

FIGURE 3: Histogram of the denaturing polyacrylamide gel shown in Figure 2. (a) Lane 2, the duplex form of the T_2AG_3 repeat. (b) Lane 4, the quadruplex form of the T_2AG_3 repeat. (c) Lane 6, the duplex form of the T_2G_4 repeat. (d) Lane 8, the quadruplex form of the T_2G_4 repeat.

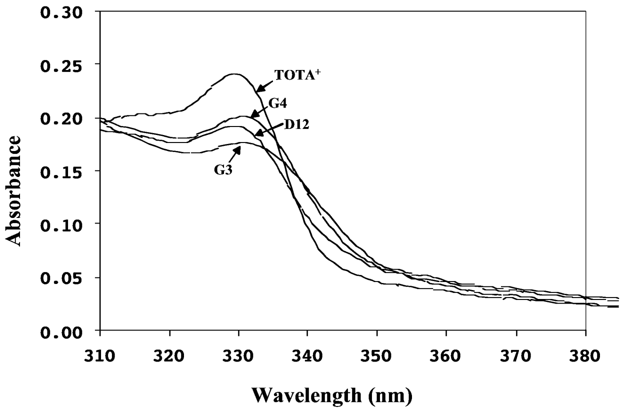

FIGURE 4: UV/vis absorption spectra of TOTA (10 μM) in 10 mM sodium phosphate buffer (pH 7) containing 100 mM KCl alone (TOTA) or in the presence of 5 μM duplex d(CGCGAATTCGCG)$_2$ (D12), quadruplex d(TTAGGGTTAGGGTTAGGGTTAGGG) (G3), or quadruplex d(TTGGGGTTGGGGTTGGGGTTGGGG) (G4).

central two guanosine residues of the 5′-GGGG-3′ sequence (Figure 3C).

TOTA-induced photochemical cleavage of the two chimeric duplex/quadruplex DNA substrates demonstrates that the T_2AG_3 and T_2G_4 repeat sequences in a quadruplex context display a different distribution of cleavage sites when compared to their duplex counterparts. In the case of the quadruplex form of the T_2AG_3 repeats, there is a general preference for cleavage of the 5′-guanosine in each of the individual 5′-GGG-3′ repeats (Figure 2, lane 4 and Figure 3B). In addition to this change in preferential photocleavage sites, the 5′-GGG-3′ repeats in the T_2AG_3 quadruplex form are less susceptible to photochemical cleavage when compared to the same repeats in a duplex context (compare Figure 2, lanes 2 and 4 and also Figure 3A,B). This resistance of quadruplex DNA to photochemical cleavage by TOTA is also clearly demonstrated in the case of the T_2G_4 repeat sequence. As shown in lane 8 of Figure 2 and also Figure 3D, the guanosine residues within the T_2G_4 repeat quadruplex are resistant to photochemical cleavage. We also examined the effect of buffer salt concentration on the resistance of guanosine residues within G-quadruplex DNA toward photochemical cleavage by TOTA. Photochemical cleavage reactions performed in the presence of 10 mM KCl gave similar results to the cleavage reactions discussed previously, which were carried out in the presence of 100 mM KCl (Supporting Information). DMS footprinting experiments demonstrated that the G-quadruplex structures were formed under both low- and high-salt conditions (Supporting Information).

Evaluation of DNA Binding Selectivity by UV/Vis Spectrophotometry and ESI-MS. To probe more deeply the properties that give TOTA its unusual reactivity, the binding selectivity of TOTA to duplex versus quadruplex DNA was evaluated by UV/vis spectrophotometry and ESI-MS. These experiments were aimed at assessing whether the apparent resistance of G-quadruplex DNA to photoinduced oxidation is simply the result of a different mode of binding of TOTA to the quadruplex as compared to duplex DNA. We also carried out spectrophotometric titrations of TOTA with various short DNA oligonucleotides including the dodecamer duplex **D12** and the intramolecular quadruplexes formed by the T_2AG_3 (**G3**) and T_2G_4 (**G4**) repeats (Figure 4). The UV/vis spectra of TOTA in the 310−380 nm region undergoes a hypochromic effect and slight bathochromic shift in the presence of the **D12** duplex, in accord with previous results employing calf thymus DNA (*25*). Both the **G3** and **G4** quadruplex structures also induce a hypochromic effect on the TOTA spectrum, and the bathochromic shift in the presence of these quadruplex structures is more pronounced than that produced in the presence of the duplex DNA. These results are also in accord with equilibrium dialysis binding studies that demonstrate TOTA binds to duplex DNA, as well as to other DNA structures such as triplex and parallel-stranded G-quadruplex DNA (*25*).

To gain more insight into the DNA binding characteristics of TOTA, we employed ESI-MS techniques. Past studies have proven ESI-MS to be successful in distinguishing drugs that selectively bind to either duplex or quadruplex DNA (*36*). For this study, a series of side-by-side experiments were undertaken in which solutions with equimolar concentrations of TOTA and either the duplex or quadruplex DNA were prepared and evaluated by ESI-MS using identical solution and instrument conditions. For the experiments involving TOTA binding to duplex oligodeoxynucleotides (ODNs), a series of three self-complementary sequences were chosen with varying amounts of A−T and G−C base pair composition (**D10A1**, **D10A2**, and **D10A3**, Table 1) so that sequence selectivity could also be examined. Figure 5 demonstrates that TOTA formed complexes with all three ODNs, with the most extensive number of complexes being formed with the duplex DNA containing greater GC content (Figure 5A,B). These results confirm past solution studies suggesting TOTA prefers binding at GC sites (*24*, *25*). Overall, TOTA readily formed complexes with the duplex DNA with duplex/TOTA binding stoichiometries ranging from 1:1 to 1:4.

Complexes formed between TOTA and quadruplex DNA were also observed in the ESI-mass spectra, as shown in Figure 6. When compared to the spectra in Figure 5 (TOTA with duplex DNA), fewer complexes are observed in the mass spectrum of the four-stranded quadruplex DNA (**G5**) with TOTA due to the high molecular weight of the complexes and the mass range limitations of the analyzer (Figure 6A). However, the range of binding stoichiometries (1:1 to 1:4) is the same in both cases. The binding of TOTA to the two-stranded quadruplex with the human telomeric sequence (**G2)** was also analyzed by ESI-MS. Figure 6B shows that TOTA also formed complexes with this quadruplex structure, with binding stoichiometries that range from 1:1 to 1:3. These results are consistent with what was observed for the duplex and **G5** structures.

Control experiments involving chromomycin were performed to demonstrate that binding selectivity can be assessed by using ESI-MS. Chromomycin is a well-characterized anticancer drug that binds to the minor groove of duplex DNA with GC base pair specificity with the requirement for a divalent metal ion. Solutions containing chromomycin, $MgCl_2$, and either duplex (**D10A1**) or quadruplex (**G5**) DNA at equimolar concentrations in 3:1 25 mM ammonium acetate/methanol were prepared. The full-scan mass spectra revealed that chromomycin formed extensive complexes with the duplex DNA, but no complexes were observed between the drug and the quadruplex DNA (spectra not shown). These results confirm that ESI-MS can be used to screen selectivity for duplex versus quadruplex

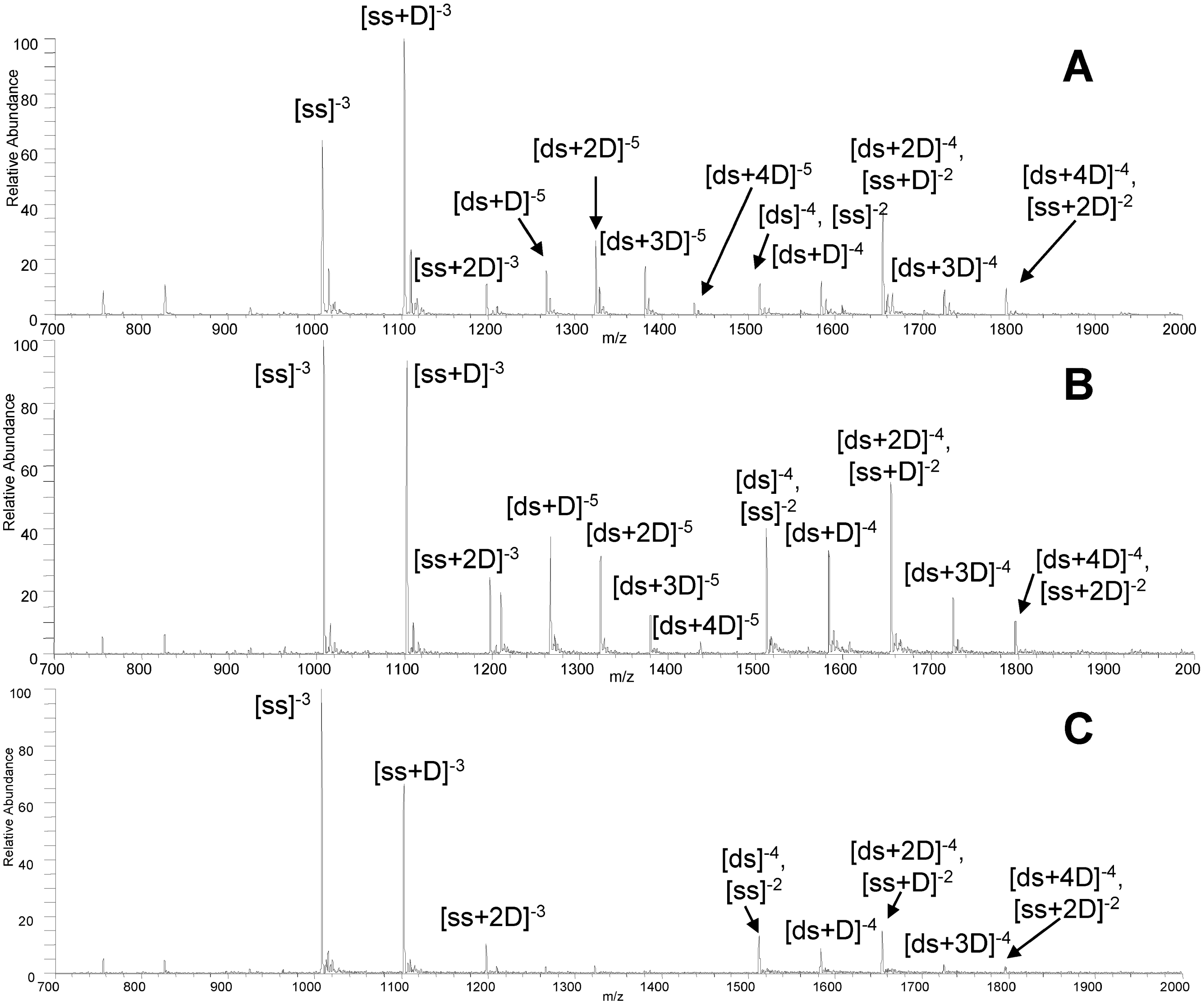

FIGURE 5: ESI-mass spectra of solutions containing TOTA with oligodeoxynucleotides (ODNs) (a) **D10A1** [5′-GCGCATGCGC-3′], (b) **D10A2** [5′-GCGATATCGC-3′], and (c) **D10A3** [5′-GCATATATGC-3′]. In each spectrum, double-stranded ODN is labeled ds, single-stranded ODN is labeled ss, and TOTA is labeled D.

DNA. Unlike chromomycin, TOTA does not exhibit such selectivity.

Evaluation of Binding Mode by ESI-MS. After the identification of TOTA/DNA complexes in solution by ESI-MS, collisional activated dissociation (CAD) experiments were undertaken on the complexes to evaluate the binding modes of TOTA. Collisional activated dissociation, in which selected gas-phase ions are energized through inelastic collisions to promote fragmentation, has been used previously to evaluate structures and relative binding energies of noncovalent complexes (*27*, *28*, *32*−*36*). Figure 7 shows examples of the characteristic fragmentation patterns observed for all of the duplex/TOTA complexes, regardless of the sequence of the ODN or the binding stoichiometry. Dissociation of the higher charge states (i.e., -5, -6) reveals that the principal fragmentation route is an unzipping of the duplex, producing single strand species both with and without retention of the TOTA molecules (Figure 7B). Strand separation is also observed in the CAD spectra of uncomplexed duplex DNA (composed of the same sequences used in this study) in the -5 charge state (spectra not shown).

For the lower charge states (i.e., -4), the dominant product ions are formed by losses of the G, A, and C nucleobases from the duplex/TOTA complexes, with less abundant ions formed by strand separation and fragmentation of the single strand backbone (Figure 7A). This mode of fragmentation has been observed in previous studies of well-studied intercalating drugs (*31*). Uncomplexed duplex DNA in the -4 charge state typically dissociates by base losses of G, A, C, and covalent cleavages along the single strand backbone but does not demonstrate strand separation (spectra not shown). Compared to the CAD spectra of the duplex DNA without bound drug, the fragmentation pattern of TOTA/duplex complexes suggests the drug is bound to the duplex in a way that weakens the Watson−Crick base pair interactions.

The CAD spectra of the quadruplex/TOTA complexes suggest a somewhat different binding mode than the duplex/TOTA complexes (Table 2). Consistent fragmentation patterns were observed for all quadruplex/TOTA complexes, as illustrated in Figure 8. These complexes dissociate via strand separation of all four strands of the quadruplex, leaving

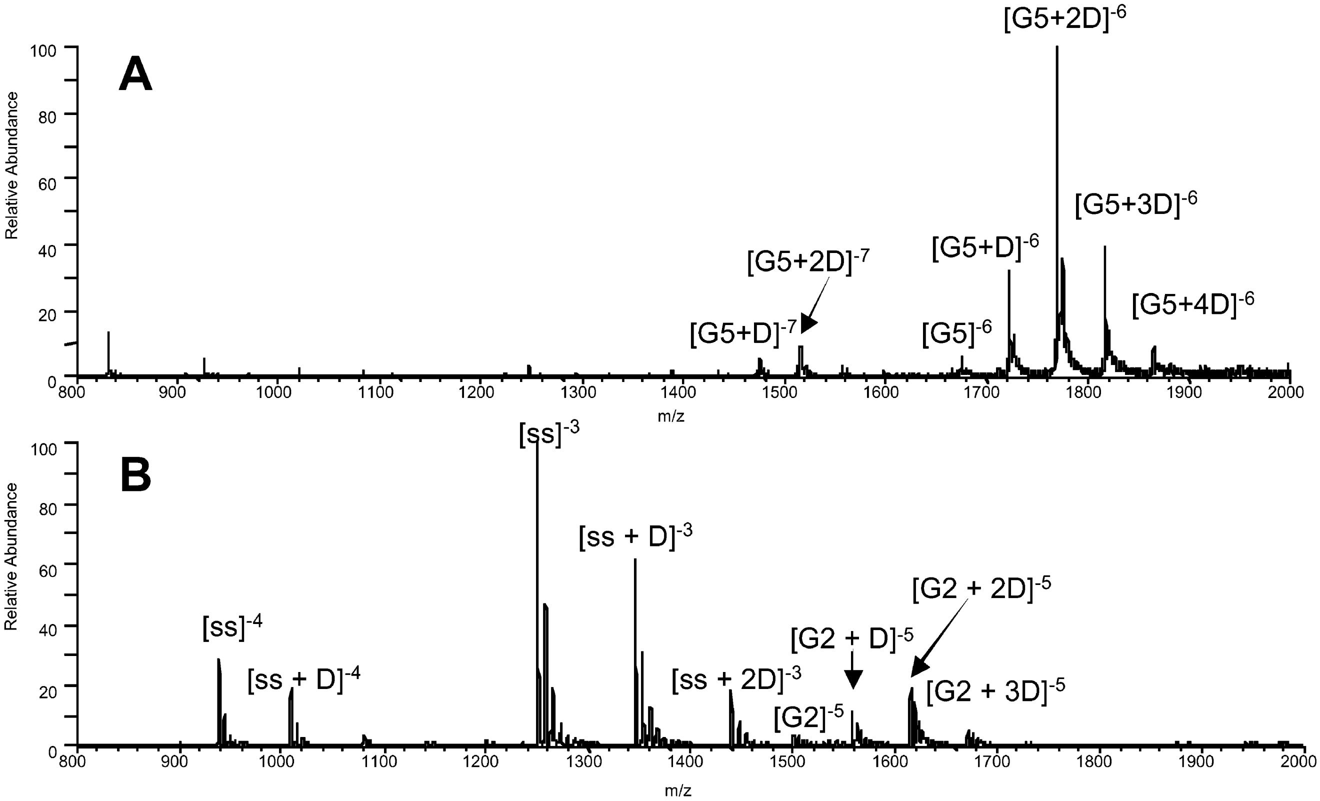

FIGURE 6: ESI-mass spectrum of a solution containing TOTA with (a) quadruplex form of **G5** [d(TTGGGGGT)$_4$] and (b) quadruplex form of **G2** [d(TTAGGGTTAGGG)$_2$]. In each spectrum, the single strand ODN is labeled ss, and TOTA is labeled D.

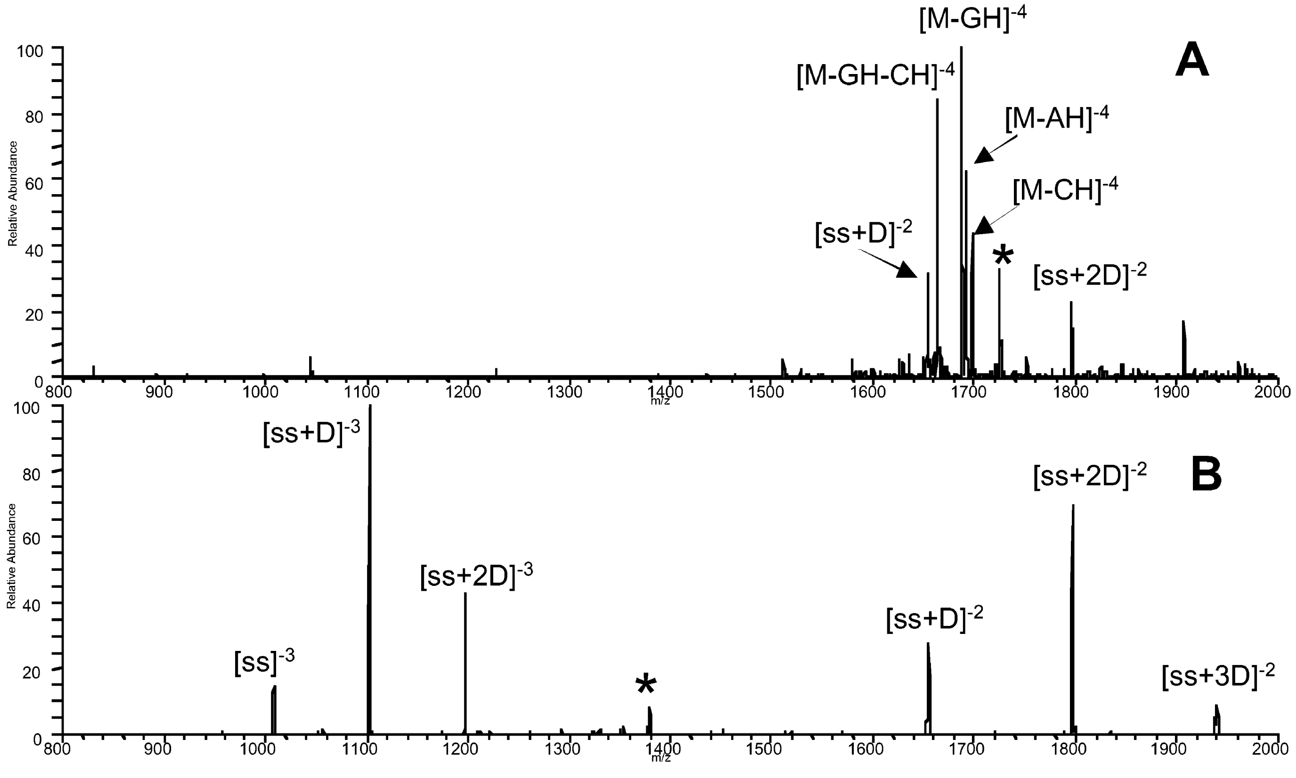

FIGURE 7: CAD product ion spectra of complexes containing double-stranded (ds) form of **D10AT** [d(GCGATATCGC)$_2$] and TOTA (D): (a) CAD of [ds + 3TOTA]$^{-4}$ and (b) CAD of [ds + 3TOTA]$^{-}$.

the intact single strand ODN, both with and without one bound TOTA molecule. However, unlike the dissociation of the duplex/TOTA complexes, the CAD spectra of the quadruplex/TOTA complexes also indicate more extensive cleavage of covalent bonds along the backbone of the ODN leading to the formation of the w_n and ($a_n - B$) ions (*43*). Product ions corresponding to a base loss of G are also observed but with much lower abundances than in the CAD

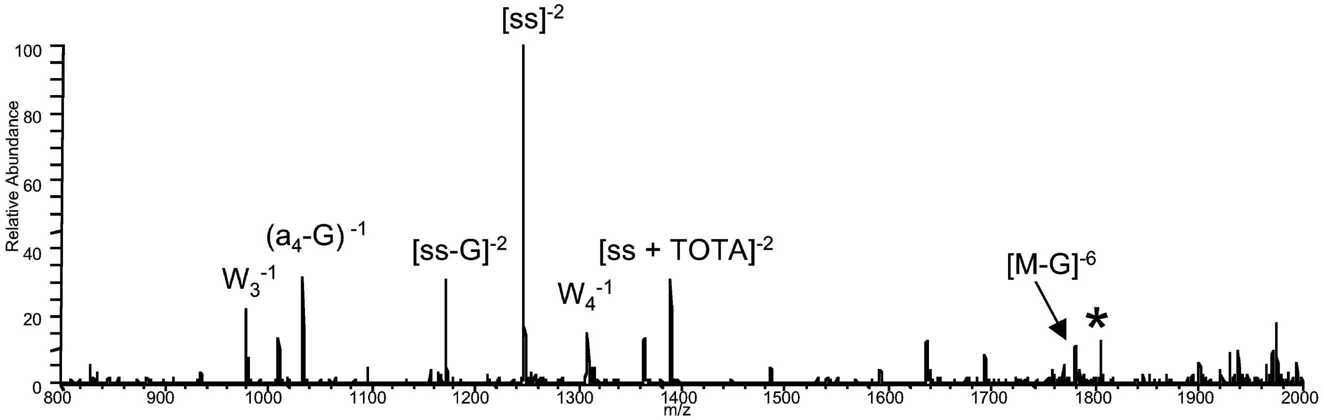

FIGURE 8: CAD product ion spectrum of the complex containing quadruplex form of **G5** [d(TTGGGGGT)$_4$] and TOTA: [G5 + 3TOTA]$^{-6}$.

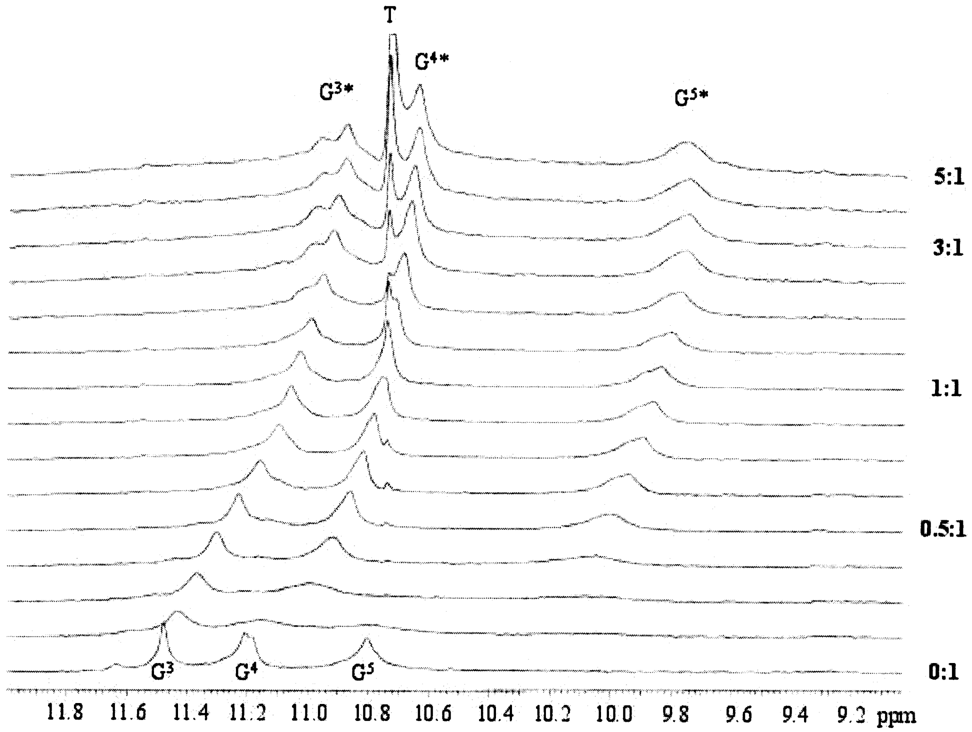

FIGURE 9: ^{1}H NMR titration of the parallel-stranded G-quadruplex form of ODN **G1** [d(TAG^{3}G^{4}G^{5}TTA)]$_4$ with TOTA. The imino proton region of the 500 MHz spectra is shown at 27 °C. The G^3, G^4, and G^5 labels indicate the imino proton G-tetrad resonances of the G-quadruplex prior to TOTA addition. With the introduction of TOTA, the imino proton resonances shift upfield (G^{3*}, G^{4*}, G^{5*}). The resonance labeled T is due to free TOTA.

spectra of the quadruplex DNA without bound TOTA. Our past study of quadruplex/ligand complexes bound by end-stacking interactions indicated that dissociation involved ejection of the drug molecule, leaving the intact quadruplex ions (*36*). The dissociation pathways of the quadruplex/TOTA complexes in the present study differ greatly from the prior reported results (*36*).

Evaluation of Binding Mode by ^{1}H NMR. To gain more insight into the difference in quadruplex interaction between TOTA and previously studied end-stacking ligands, we carried out NMR studies of the complex formed between TOTA and the parallel-stranded G-quadruplex formed from ODN **G1** (Table 1). We have previously reported NMR-derived structural models for the interaction of perylene diimides with the quadruplex form of **G1** (*26*, *44*). The perylene diimides stack upon the 3′-proximal G-tetrad of the **G1** quadruplex, and the formation of these complexes is accompanied by a distinctive upfield shift of the imino proton resonance for the 3′-proximal G-tetrad (*26*, *44*).

Titrating a solution of TOTA into the quadruplex form of **G1** results in a pronounced broadening and upfield shift of the imino proton resonance of the 3′-proximal G-tetrad (Figure 9). The imino proton resonances of the central and 5′-proximal G-tetrads undergo more modest upfield shifts. The direction and magnitude of these chemical shifts is very similar to those observed in the 3′-end stacking of perylene diimides to this quadruplex (*26*, *44*). However, the free and perylene diimide-bound forms of the quadruplex can be clearly distinguished in the NMR, indicative of slow exchange between these forms, whereas only a single set of imino proton resonances are apparent upon addition of up to 1 equiv of TOTA to the quadruplex. The apparent fast exchange between the free and the TOTA-bound forms of the quadruplex may be due to the somewhat weaker binding of TOTA, relative to the perylene diimides. This relatively weak binding is also evident by the resonance arising from free TOTA that can be seen even after the addition of less than 1 equiv of TOTA to the quadruplex (marked T in Figure 9). Quantifying the TOTA-induced chemical shifts using the method of Correia and co-workers (*45*), we calculate a G-quadruplex association constant for TOTA of $1.3 \pm 0.3 \times 10^4\ M^{-1}$. This relative weak binding is similar to that reported for TOTA binding to double-stranded calf thymus DNA (*25*). The addition of excess TOTA to the quadruplex results in further upfield shifts in the imino proton resonances, and the appearance of additional imino resonances that may be due to the formation of higher-order TOTA—quadruplex complexes.

DISCUSSION

The stable trioxatriangulenium ion TOTA has been reported to bind with little selectivity to many DNA structures including duplex, triplex, and quadruplex DNA (*24*, *25*). Here, we have investigated the binding interactions between TOTA and duplex and quaduplex DNA using ESI-MS. We find that TOTA has a preference for binding to duplexes with high GC base-pair content, and CAD results suggest that the TOTA binds to duplex DNA via intercalation but that this binding causes distortions in the duplex structure that facilitate fragmentation by strand separation. These results are in accord with previous reports of duplex DNA—TOTA intercalative complexes in which there is an unusually large degree of DNA unwinding at the intercalation site (*25*).

The interaction between TOTA and various G-quadruplex DNA structures was also investigated. UV/vis spectroscopic titrations indicate that TOTA interacts with intramolecular G-quadruplex DNA structures formed by telomeric T_2AG_3 and T_2G_4 repeats. ESI-MS studies demonstrate that TOTA binds to the four-stranded G-quadruplex DNA structure formed by the T_2G_5T sequence and the two-stranded structure containing the $T_2AG_3T_2AG_3$ sequence. The binding stoichiometry and fragmentation of the quadruplex—TOTA complexes are unlike that observed for G-quadruplex ligands that bind by G-tetrad end-stacking. NMR titrations carried out with a parallel-stranded G-quadruplex provide support for an initial end-stacking mode of binding, although other binding modes may be involved in the formation of higher-order complexes.

Despite the ability of TOTA to bind to both duplex and G-quadruplex DNA structures, the photochemical cleavage of duplex telomeric repeats by TOTA occurs more readily than photocleavage of these repeats in a G-quadruplex DNA form. The resistance of G-quadruplex DNA to TOTA photocleavage contrasts with previous reports of enhanced oxidation of intramolecular T_2AG_3 G-quadruplex structures with free or covalently attached transition metal complexes (*10*, *11*). The binding of multiple TOTA ligands to the DNA structures may impede the long-range electron transport between duplex and quadruplex DNA that has been observed in these previous reports. Further studies of the relative ease of oxidation of G-quadruplex versus duplex DNA structures that take into account the role of different oxidants and their binding modes as well as the specific sequence, structure, and stability of the G-quadruplex DNA will provide insights and lead to a clearer understanding of the potential role of these DNA structures in modulating oxidative DNA damage at telomeric or other DNA regions.

SUPPORTING INFORMATION AVAILABLE

Experimental procedures and data for DMS footprinting and salt-dependent photochemical cleavage reactions. This material is available free of charge via the Internet at http://pubs.acs.org.

REFERENCES

1. Delaney, S., and Barton, J. K. (2003) Long-range DNA charge transport, *J. Org. Chem. 68*, 6475—6483.
2. Lewis, F. D., Liu, J., Weigel, W., Rettig, W., Kurnikoc, I. V., and Bertan, D. N. (2002) Donor—bridge—acceptor energetics determine the distance dependence of electron tunneling in DNA, *Proc. Natl. Acad. Sci. U.S.A. 99*, 12536—12541.
3. Giese, B. (2002) Electron transfer in DNA, *Curr. Opin. Chem. Biol*. *6*, 612—618.
4. (a) Hall, D. B., and Barton, J. K. (1997) Sensitivity of DNA-mediated electron transfer to the intervening pi-stack: A probe for the integrity of the DNA base stack, *J. Am. Chem. Soc. 119*, 5045—5046. (b) Gasper, S. M., and Schuster, G. B. (1997) Intramolecular photoinduced electron transfer to anthraquinones linked to duplex DNA: The effect of gaps and traps on long-range radical cation migration, *J. Am. Chem. Soc. 119*, 12762—12771.
5. (a) Ly, D., Kan, Y., Armitage, B., and Schuster, G. B. (1996) Cleavage of DNA by irradiation of substituted anthraquinones: Intercalation promotes electron transfer and efficient reaction at GG steps, *J. Am. Chem. Soc. 118*, 8747—8748. (b) Breslin, D. T., and Schuster, G. B. (1996) Anthraquinone photonucleases: Mechanisms for GG-selective and nonselective cleavage of double-stranded DNA, *J. Am. Chem. Soc. 118*, 2311—2319. (c) Nuñez, M. E., Hall, D. B., and Barton, J. K. (1999) Long-range oxidative damage to DNA: effects of distance and sequence, *Chem. Biol. 6*, 85—97. (d) Sartor, V., Boone, E., and Schuster, G. B. (2001) Long-distance radical cation migration through A/T base pairs in DNA: An experimental test of theory, *J. Phys. Chem. B. 105*, 11057—11059.
6. (a) Armitage, B. (1998) Photocleavage of nucleic acids, *Chem. Rev. 98*, 1171—1200. (b) Schuster, G. B. (2000) Long-range charge transfer in DNA: Transient structural distortions control the distance dependence, *Acc. Chem. Res. 33*, 253—260.
7. (a) Ito, K., and Kawanishi, S. (1997) Photoinduced hydroxylation of deoxyguaniosine in DNA by Pterins: Sequence specificity and mechanism, *Biochemistry 36*, 1774—1781. (b) Yoshioka, Y., Kitgawa, Y., Takano, Y., Yamaguchi, K., Nakamura, T., and Saito, I. (1999) Experimental and theoretical studies on the selectivity of GGG triplets toward one-electron oxidation in B-form DNA, *J. Am. Chem. Soc. 121*, 8712—8719. (c) Sanii, L., and Schuster, G. B. (2000) Long-distance charge transport in DNA: Sequence-dependent radical cation injection efficiency, *J. Am. Chem. Soc. 122*, 11545—11546.
8. Núñez, M. E., Noyes, K. T., Gianolio, D. A., McLaughlin, L. W., and Barton, J. K. (2000) Long-range guanine oxidation in DNA restriction fragments by a triplex-directed naphthalene diimide intercalator, *Biochemistry 39*, 6190—6199.
9. Odom, D. T., Dill, E. A, and Barton, J. K. (2001) Charge transport through DNA four-way junctions, *Nucleic Acids Res. 29*, 2026—2033.
10. Delaney, S., and Barton, J. K. (2003) Charge transport in DNA duplex/quadruplex conjugates, *Biochemistry 42*, 14159—14165.
11. Szalai, V. A., and Thorp, H. H. (2000) Electron transfer in tetrads: Adjacent guanines are not hole traps in G quartets, *J. Am. Chem. Soc. 122*, 4524—4525.
12. Freidman, K. A., and Heller, A. (2001) Guanosine distribution and oxidation resistance in eight eukaryotic genomes, *J. Phys. Chem*. 105, 11859—11865.
13. Blackburn, E. H. (1991) Structure and function of telomeres, *Nature 350*, 569—573.
14. Counter, C. M. (1996) The roles of telomeres and telomerase in cell life span, *Mutat. Res. 366*, 45—63.
15. Oikawa, S., Tada-Okinawa, S., and Kawanishi, S. (2001) Site-specific DNA damage at the GGG sequence by UVA involves acceleration of telomere shortening, *Biochemistry 40*, 4763—4768.

16. Kerwin, S. M. (2000) G-quadruplex DNA as a target for drug design, *Curr. Pharm. Des. 6*, 441−471.
17. Schaffitzel, C., Berger, I., Postberg, J., Hanes, J., Lipps, H. J., and Plückthun, A. (2001) In vitro generated antibodies specific for telomeric guanine-quadruplex DNA react with *Stylonychia lemnae* macronuclei, *Proc. Natl. Acad. Sci. U.S.A. 98*, 8572−8577.
18. Henderson, E., Hardin, C. C., Wolk, S. K., Tinoco, I. Jr., and Blackburn, E. H. (1987) Telomeric DNA oligonucleotides form novel intramolecular structures containing guanine guanine base-pairs, *Cell 51*, 899−908.
19. Siddiqui-Jain, A., Grand, C. L., Bearss, D. J., and Hurley L. H. (2002) Direct evidence for a G-quadruplex in a promoter region and its targeting with a small molecule to repress c-MYC transcription, *Proc. Natl. Acad. Sci. U.S.A. 99*, 11593−11598.
20. Greider, C. W. (1999) Telomeres do d-loop-t-loop, *Cell 97*, 419−422.
21. Reynisson, J., Balakrishnan, G., Wilbrandt, R., and Harrit, N. (2000) Vibrational spectroscopic and quantum chemical studies of the trioxatriangulenium carbocation, *J. Mol. Struct. 520*, 63−73.
22. Krebs, F. C., Laursen, B. W., Johannsen, I., Faldt, A., Bechgaard, K., Jacobsen, C. S., Thorup, N., and Boubekeur, K. (1998) The geometry and structural properties of the 4,8,12-trioxa-4,8,12,12c-tetrahydrodibenzo[*cd*, *mn*]pyrene system in the cationic state. Structures of a planar organic cation with various monovalent and divalent anions, *Acta Crystallogr., Sect. B 55*, 410−423.
23. Dileesh, S., and Gopidas, K. R. (2000) Photophysical and electron-transfer studies of a stable carbocation, *Chem. Phys. Lett. 330*, 397−402.
24. Pothukuchy, A., Ellapan, S., Gopidas, K. R., and Salazar, M. (2003) Photooxidatio of duplex DNA with the stable trioxatriangulenium ion, *Bioorg. Med. Chem. Lett. 13*, 1491−1494.
25. Reynisson, J., Schuster, G. B., Howerton, S. B., Williams, L. D., Barnett, R. N., Cleveland, C. L., Landman, U., Harrit, N., and Chaires, J. B. (2003) Intercalation of trioxatriangulenium ion in DNA: Binding, electron transfer, X-ray crystallography, and electronic structure, *J. Am. Chem. Soc. 125*, 2072−2083.
26. Kern, J. T., Thomas, P. W., and Kerwin, S. M. (2002) The relationship between ligand aggregation and G-quadruplex DNA selectivity in a series of 3,4,9,10-perylenetetracarboxylic acid diimides, *Biochemistry 41*, 11379−11389.
27. Hofstadler, S. A., and Griffey, R. H. (2001) Analysis of non-covalent complexes of DNA and RNA by mass spectrometry, *Chem. Rev. 101*, 377−390.
28. Beck, J. L., Colgrave, M. L., Ralph, S. F., and Sheil, M. M. (2001) Electrospray ionization mass spectrometry of oligonucleotide complexes with drugs, metals, and proteins, *Mass Spectrom. Rev. 20*, 61−87.
29. Busch, K. L., Glish, G. L., and McLuckey, S. A. (1988) *Mass Spectrometry/Mass Spectrometry: Techniques and Applications of Tandem Mass Spectrometry*, VCH Publishers: New York.
30. Gale, D. C., and Smith, R. D. (1995) Characterization of noncovalent complexes formed between minor groove binding molecules and duplex DNA by electrospray ionization mass spectrometry, *J. Am. Soc. Mass Spectrom. 6*, 1154−1164.
31. Wan, K. X., Gross, M. L., and Shibue, T. (2000) Gas-phase stability of double-stranded oligodeoxynucleotides and their noncovalent complexes with DNA-binding drugs as revealed by collisional activation in an ion trap, *J. Am. Soc. Mass Spectrom. 11*, 450−457.
32. Gabelica, V., Rosu, F., Houssier, C., and De Pauw, E. (2000) Gas phase thermal denaturation of an oligonucleotide duplex and its complexes with minor groove binders, *Rapid Commun. Mass Spectrom. 14*, 464−467.
33. Wan, K. X., Shibue, T., and Gross, M. L. (2000) Noncovalent complexes between DNA-binding drugs and double-stranded oligodeoxynucleotides: A study by ESI ion-trap mass spectrometry, *J. Am. Chem. Soc. 122*, 300−307.
34. Gabelica, V., De Pauw, E., and Rosu, F. (1999) Interaction between antitumor drugs and a double-stranded oligonucleotide studied by electrospray ionization mass spectrometry, *J. Mass. Spectrom. 34*, 1328−1337.
35. Carrasco, C., Rosu, F., Gabelica, V., Houssier, C., De Pauw, E., Garbay-Jaureguiberry, C., Roques, B., Wilson, W. D., Chaires, J. B., Waring, M. J., and Bailly, C. (2002) Tight binding of the antitumor drug ditercalinium to quadruplex DNA, *ChemBiochem 3*, 1235−1241.
36. David, W. M., Brodbelt, J., Kerwin, S. M., and Thomas, P. W. (2002) Investigation of quadruplex oligonucleotide−drug interactions by electrospray ionization-mass spectrometry, *Anal. Chem. 74*, 2029−2033.
37. Guittat, L., Alberti, P., Rosu, F., Van Miert, S., Thetiot, E., Pieters, L., Gabelica, V., De Pauw, E., Ottaviani, A., Riou, J. F., and Mergny, J. L. (2003) Interactions of cryptolepine and neocryptolepine with unusual DNA structures, *Biochimie 85*, 535−547.
38. Rosu, F., De Pauw, E., Guittat, L., Alberti, P., Lacroix, L., Mailliet, P., Riou, J. F., and Mergny, J. L. (2003) Selective interaction of ethidium derivatives with quadruplexes: An equilibrium dialysis and electrospray ionization mass spectrometry analysis, *Biochemistry 42*, 10361−10371.
39. Rosu, F., Gabelica, V., Shin-ya, K., and De Pauw, E. (2003) Telomestatin-induced stabilization of the human telomeric DNA quadruplex monitored by electrospray mass spectrometry, *Chem. Commun.* 2702−2703.
40. Plateau, P., and Gueron, M. (1982) Exchangeable proton NMR without baseline distortion, using new strong-pulse sequences, *J. Am. Chem. Soc. 104*, 7310−7311.
41. (a) Tuntiwechapikul, W., Lee, J. T., and Salazar, M. (2001) Design and synthesis of the G-quadruplex-specific cleavage reagent perylene-EDTA•Iron(II), *J. Am. Chem. Soc. 123*, 5606−5607. (b) Tuntiwechapikul, W., and Salazar, M. (2001) Cleavage of G-quadruplex DNA with perylene-EDTA•Fe(II), *Biochemistry 40*, 13652−13658.
42. Henderson, P. T., Jones, D., Hampikian, G., Kan, Y., and Schuster, G. B. (1999) Long-distance charge transport in duplex DNA: The phonon-assisted polaron-like hopping mechanism, *Proc. Natl. Acad. Sci. U.S.A. 96*, 8353−8358.
43. McLuckey, S. A., Van Berkel, G. J., and Glish, G. L. (1991) Tandem mass-spectrometry of small, multiply charged oligonucleotides, *J. Am. Soc. Mass Spectrom. 3*, 60−70.
44. Oleg, Yu., Fedoroff, O. Y., Miguel Salazar, M., Haiyong Han, H., Chemeris, V. V., Kerwin, S. M., and Hurley, L. H. (1998) NMR-based model of a telomerase-inhibiting compound bound to G-quadruplex DNA, *Biochemistry 37*, 12367−12374.
45. Correia, I., Bezzenine, N., Ronzani, N., Platzer, N., Beloil, J. C., and Doan, B. T. (2002) Study of inclusion complexes of acridine with β- and (2,6-di-*O*-methyl)-β-cyclodextrin by use of solubility diagrams and NMR spectroscopy, *J. Phys. Org. Chem. 15*, 647−659.

BI0485981